THE JOURNAL OF PHYSICAL CHEMISTRY C LETTERS

2009, *113,* 5902–5905
Published on Web 03/25/2009

Morphology Instability of Silicon Nitride Nanowires

Huatao Wang,[†] Weiyou Yang,[‡] Zhipeng Xie,*[,†] Yansong Wang,[$] Feng Xing,[||] and Linan An*[,§]

State Key Laboratory of New Ceramics and Fine Processing, Department of Materials Science and Engineering, Tsinghua University, Beijing, 100084, China, Institute of Materials, Ningbo University of Technology, Ningbo 315016, China, Optical Tech Research Center, Changchun Institute of Optics, Fine Mechanics and Physics, Chinese Academy of Science, Changchun 130032, China, The Key Laboratory on Durability of Civil Engineering in Shenzhen, Shenzhen University, Shenzhen 518060, China, and Advanced Materials Processing and Analysis Center, University of Central Florida, Orlando, Florida 32816

Received: March 3, 2009; Revised Manuscript Received: March 19, 2009

We report that cylinder-shaped Si_3N_4 nanowires are not stable and can gradually transform into nanobelts via surface diffusion during high-temperature annealing. We demonstrate that such instability is driven by the requirements for reducing overall surface energy. The resultant nanobelts have the same width-to-thickness ratio, suggesting a stable morphology. A model in terms of surface energy is proposed to explain the formation of such stable morphology, which agrees well with experimental results. Our result suggests that instability could be a limiting factor for high-temperature applications of 1D nanostructures.

1. Introduction

Recently, one-dimensional (1D) nanostructures have gained considerable attention because of their potential applications in nanoscaled electronics,[1−3] optoelectronics,[4−6] and sensors.[7,8] In the last 15 years or so, tremendous effort has been devoted to develop a variety of techniques to control the morphology of the synthesized 1D nanostructures since it is generally believed that the morphology plays a key role in determining their properties and applications.[9−11] 1D nanostructures with different morphologies such as cylinder-shaped nanowires, prism-shaped nanowires, and nanobelts (rectangular-shaped cross-section) have been successfully synthesized.[12−14] The formation of different morphologies was determined by thermodynamic/kinetic conditions of the synthesis processes.[15−17] However, these conditions generally no longer exist in the environments where the nanostructures will be used. Consequently, whether these morphologies are stable during their usage becomes an important issue, which has received little attention. This is more relevant when the nanostructures are used at high temperatures, where the mobility of atoms is high enough for achieving a new equilibrium under new thermodynamic conditions.

Here, we show that the cylinder-shaped silicon nitride (Si_3N_4) nanowires are not stable and can be gradually evolved into nanobelts during high-temperature annealing. Silicon nitride is an important wide-band gap semiconductor with a band gap of 5.0 eV.[18] Similar to III−N semiconductors (e.g., GaN and AlN), Si_3N_4 possesses outstanding thermal/mechanical properties, chemical inertness, and high doping concentration[19−21] and, thus, could be an excellent host material. Recently, synthesis of Si_3N_4 nanostructures has been extensively explored because of their potential applications in high temperature and short wavelength nanodevices.[22−24] Due to its unique hexagonal structure, the surface energy significantly varies for different crystallographic planes, which determines the growth habits of Si_3N_4.[25] In this paper, we demonstrate that such differences in surface energies can cause a morphology instability and transformation and determine the final shape of the nanobelts.

2. Experimental Methods

The Si_3N_4 nanowires used in this study were synthesized by catalyst-assisted pyrolysis of a commercially available polysilazane.[26] First, the liquid precursor was solidified by heat-treatment at 260 °C for 0.5 h in ultrahigh purity nitrogen. The obtained solid was then crushed into a fine powder by high-energy ball milling, with ∼1 wt % $Fe(NO_3)_3$ powder being added as the catalyst. The powder mixture was then placed in a high-purity alumina crucible and pyrolyzed in a tube furnace at 1350 °C for 3 h in flowing ultrahigh-purity nitrogen at 0.1 MPa, followed by furnace cooling to room temperature. The obtained products are hexagonal-phased α-Si_3N_4 nanowires with a cylinder shape (Figure 1a), which are ∼50−200 nm in diameter and up to several hundred micrometers long.[26] The formation of cylinder-shaped nanowires was attributed to a solid−liquid−gas−solid (SLGS) process.[26]

The obtained Si_3N_4 nanowires were separated from the pyrolysis residues using ultrasonic purification and then placed into the tube furnace and annealed at 1450 °C in flowing ultrahigh-purity nitrogen of 0.1 MPa for different times. The annealed nanowires were then analyzed using scanning electron microscopy (SEM) and transmission electron microscopy (TEM).

3. Results and Discussion

The nanowires annealed at different times were first observed by scanning electron microscopy to evaluate their stability and

* To whom corresponding should be addressed. E-mail: xzp@mail.tsinghua.edu.cn (Z.X.); lan@mail.ucf.edu (L.A.).
[†] Tsinghua University.
[‡] Ningbo University of Technology.
[$] Chinese Academy of Science.
[||] Shenzhen University.
[§] University of Central Florida.

10.1021/jp901938a CCC: $40.75

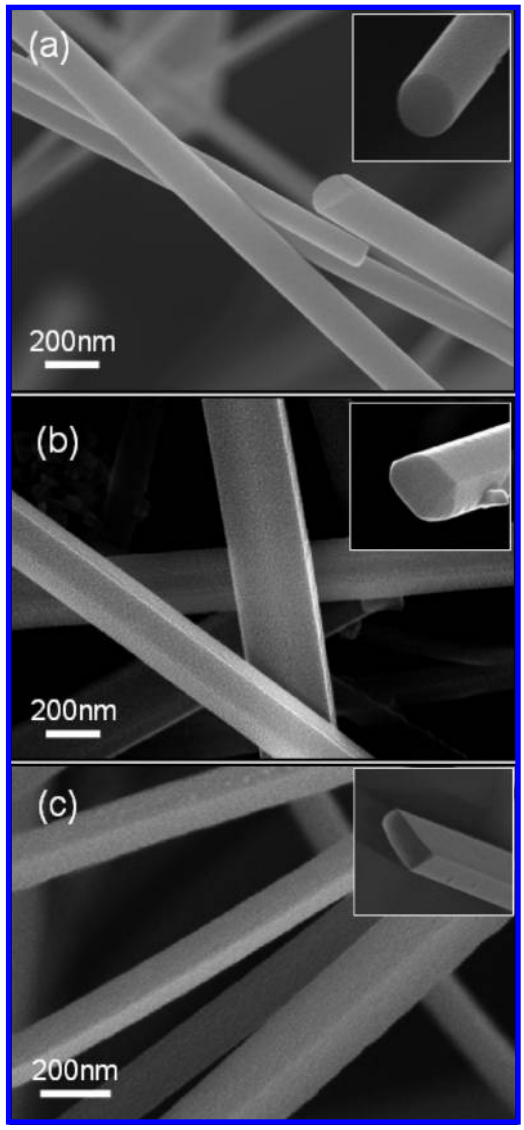

Figure 1. Scanning electron microscopy images of (a) as-received cylinder-shaped nanowires, (b) prism-shaped nanowires obtained after annealing at 1450 °C for 10 min, and (c) nanobelts after annealing at 1450 °C for 120 min. The inserts are respective cross-section morphologies of the nanostructures at each stage.

morphology evolution (Figure 1). The results clearly reveal that the cylinder shape of the original Si_3N_4 nanowires is not stable, and transformed first into prism-shaped nanowires (Figure 1b), and then into nanobelts (Figure 1c). There is no clear evidence for any volume change during the shape evolution. This can be understood since the very low vapor pressure of Si_3N_4 at the annealing temperature. The transformation is thus via surface diffusion. It is interesting to note that further increasing annealing time (after ~100 min), the shape (width-to-thickness ratio) of the nanobelts remains the same, suggesting that the shape of the nanobelts is thermodynamically stable.

To further investigate the morphology instability and transformation, the structure of the stable nanobelts has been analyzed by transmission electron microscopy and electron diffraction. The results reveal that the nanobelts remain α-Si_3N_4 in phase and no phase transformation accompanied morphology changes, which is confirmed by XRD analysis on both the nanowires and nanobelts. Analysis of more than ten nanobelts reveals that there are only two kinds of nanobelts, with their axial directions along [100] (Figure 2a) and [101] (Figure 2b), respectively. The nanowires and nanoprisms exhibit the same SAED patterns, suggesting that the growth directions remain the same during annealing. Further analysis of the TEM images and the diffraction patterns reveals that the nanobelts with their axis along the [100] direction have $\{\bar{1}20\}$ and {001} as width and thickness surfaces (Figure 2c), respectively, whereas the nanobelts with their axis along the [101] direction have $\{\bar{1}20\}$ and $\{\bar{1}01\}$ as width and thickness surfaces (Figure 2d), respectively.

The observed morphology instability and transformation of the Si_3N_4 nanowires are driven by the requirement for reducing surface energy. The nanowires with a cylinder shape unavoidably contain energetically unfavorable high-index surfaces. During the synthesis, formation of such an energetically unstable cylinder shape is due to the confining effect of the catalytic droplets, where the boundary between the nanowires and the droplet tends to be circular to minimize surface energy. However, such confinement no longer exists during annealing. Atoms on high-energy surfaces tend to rearrange onto low-index surfaces which have lower energies to form faceted morphology. α-Si_3N_4 has a lattice parameter ratio of c/a = 0.725 (JCPDS Card No. 41−0360), which is less than that of the ideal close-packed hexagonal structure (c/a = 1.633). As a result, its $\{\bar{1}20\}$ planes have the highest packing density and lowest surface energy,[25] similar to other hexagonal structures.[27] Consequently, during annealing (when the temperature is high enough), atoms rearranged onto $\{\bar{1}20\}$ planes and grew the planes to form the width surface. This is consistent with experimental observations (Figure 2). With axial directions and width surfaces being fixed (by the growing direction of the original nanowires), the thickness surfaces of the nanobelts were automatically determined, to be {001} (Figure 2c) and $\{\bar{1}01\}$ (Figure 2d), respectively.

The formation of the stable nanobelts (fixed aspect ratio of width-to-thickness) is a direct result of minimizing surface energy. Considering a nanobelt with unit length, the volume, V, of the nanobelt is given by

$$V = wt \tag{1}$$

where w and t are width and thickness of the nanobelts, respectively. During morphology change, the volume remains constant (neglecting the evaporation of Si_3N_4 due to its low vapor pressure at annealing temperature). The total surface energy, U_s, of the nanobelt is

$$U_s = 2(w\gamma_w + t\gamma_t) \tag{2}$$

where γ_w and γ_t are respective specific surface energies of width and thickness, and are constants for given crystallographic planes. Combining eqs 1 and 2

$$U_s = 2\left(w\gamma_w + \frac{V}{w}\gamma_t\right) \tag{3}$$

Taking the derivative of eq 3 and equating it to zero (since the surface energy is to be minimized), we obtain the following relationship:

$$\frac{\partial U_s}{\partial w} = 2\left(\gamma_w - \frac{V\gamma_t}{w^2}\right) = 0 \tag{4}$$

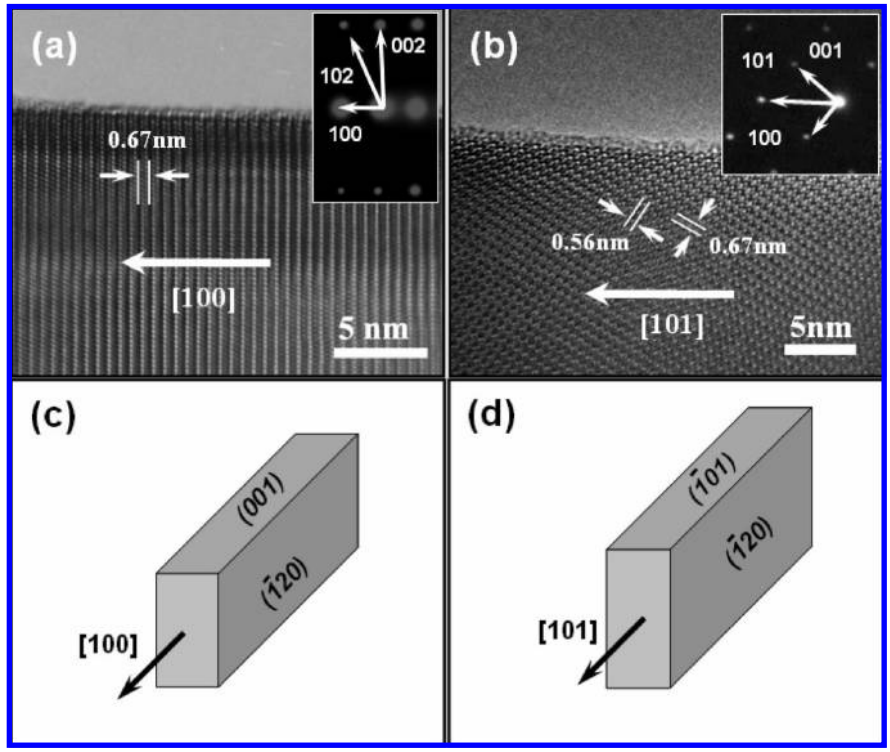

Figure 2. (a and b) Transmission electron microscopy images of nanobelts grown along [100] and [101] directions, respectively. The insets are corresponding selected area electron diffraction patterns. (c and d) Schematic models of the characteristic surfaces of the nanobelts shown in panels a and b, respectively.

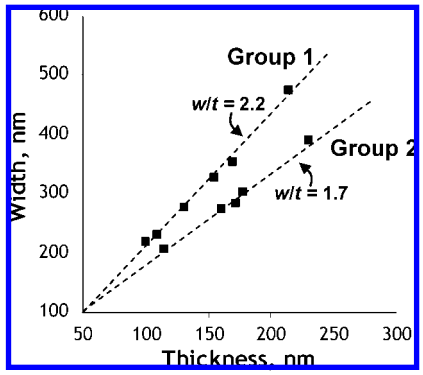

Figure 3. Linear relationship between the width and thickness of the Si_3N_4 nanobelts.

Combining eqs 1 and 4, we obtain the final result:

$$w = \frac{\gamma_t}{\gamma_w} t \tag{5}$$

This suggests that the width and thickness of an equilibrium nanobelt should have linear relationship; its aspect ratio (w/t) should be equal to the surface energy ratio of γ_t/γ_w.

To test the above analysis, we measured the width and thickness of the nanobelts under SEM, and plot them in Figure 3. It is interesting to see that the data splits into two groups; and within each group, the width and the thickness of the nanobelts exhibit well-defined linear relationships. This is consistent with the prediction of eq 5 and the experimental result which reveals that there are two types of nanobelts with different facets (Figure 2). The current result shown in Figure 3 suggests that $\gamma_{\bar{1}01}/\gamma_{\bar{1}20}$ should be 2.2 (the nanobelts along [101] direction) and $\gamma_{001}/\gamma_{\bar{1}20}$ should be 1.7 (the nanobelts along [100] direction).

Krämer et al. have calculated the surface energies of various crystallographic planes for the hexagonal Si_3N_4 in a supercooled liquid using the periodic bond chain method, and obtained $\gamma_{\bar{1}01}/\gamma_{\bar{1}20} = 3.0$ and $\gamma_{001}/\gamma_{\bar{1}20} = 2.0$.[25] Note that these calculations accounted for the inherent properties at room temperature; while the morphology change reported here was carried out at the elevated temperature. Surface energies are affected by temperature. Generally, increasing temperature will lead to the decrease in the difference between the surface energies of different planes.

To further test the thermodynamic model discussed above, α-Si_3N_4 nanobelts synthesized using the procedure described in ref 28 are annealed at the same conditions. These nanobelts also grew along either [100] or [101] directions and have the aspect ratios of 8−10,[28] which is much higher than the stable value as predicted above. It is interesting to note that the *w*-to-*t* ratio (morphology) of the nanobelts remains the same, and does not change to the stable value. This can be understood as follows. For nanobelts of high aspect ratios changing to the stable shape of the low aspect ratio, atoms on the lower-energy $\{\bar{1}20\}$ surface need to move to the higher-energy $\{001\}/\{\bar{1}01\}$ surfaces. Although the total surface energy will be reduced by the change of morphology (eq 5), the local energy barriers prevent such motion of atoms, leading to that the nanobelts stayed in their metastable shapes. This suggests that nanobelts with the aspect ratio higher than the equilibrium value can retain their shapes.

4. Conclusion

In summary, morphology instability and transformation of cylinder-shaped Si_3N_4 nanowires are experimentally observed. During high-temperature annealing, the original nanowires gradually transform into nanobelts with stable shapes. We have proposed a thermodynamic origin which can consistently explain the occurrence of such morphology changes. Since the instability

is the result of minimizing surface energies, it could happen at even lower temperatures by taking longer times. Our result suggests that thermal stability could be a limiting factor for applying 1D nanostructures at relatively high temperatures.

Acknowledgment. The work is financially supported by the National Science Foundation of China (Nos. 50372031 and 50872058), the two-based projects of NSFC (No. 50540420104), the Specialized Research Foundation for the Doctoral program of Higher Education (No. 20050003004), and International Cooperation Project of Ningbo Municipal Government (Grant No. 2008B10044).

References and Notes

(1) Cui, Y.; Lieber, C. M. *Science* **2001**, *291*, 851.
(2) Cui, Y.; Zhong, Z. H.; Wang, D. L.; Wang, W. U.; Lieber, C. M. *Nano Lett.* **2003**, *3*, 149.
(3) De Franceschi, S.; van Dam, J. A.; Bakkers, E.; Feiner, L. F.; Gurevich, L.; Kouwenhoven, L. P. *Appl. Phys. Lett.* **2003**, *83*, 344.
(4) Haraguchi, K.; Katsuyama, T.; Hiruma, K.; Ogawa, K. *Appl. Phys. Lett.* **1992**, *60*, 745.
(5) Duan, X. F.; Huang, Y.; Cui, Y.; Wang, J. F.; Lieber, C. M. *Nature (London)* **2001**, *409*, 66.
(6) Wang, J. F.; Gudiksen, M. S.; Duan, X. F.; Cui, Y.; Lieber, C. M. *Science* **2001**, *293*, 1455.
(7) Comini, E.; Faglia, G.; Sberveglieri, G.; Pan, Z. W.; Wang, Z. L. *Appl. Phys. Lett.* **2002**, *81*, 1869.
(8) Kong, J.; Franklin, N. R.; Zhou, C. W.; Chapline, M. G.; Peng, S.; Cho, K. J.; Dai, H. J. *Science* **2000**, *287*, 622.
(9) Herricks, T.; Chen, J. Y.; Xia, Y. N. *Nano Lett.* **2004**, *4*, 2367.
(10) Pinna, N.; Weiss, K.; Urban, J.; Pileni, M. P. *Adv. Mater.* **2001**, *13*, 261.
(11) Yu, S. H.; Wu, Y. S.; Yang, J.; Han, Z. H.; Xie, Y.; Qian, Y. T.; Liu, X. M. *Chem. Mater.* **1998**, *10*, 2309.
(12) Morales, A. M.; Lieber, C. M. *Science* **1998**, *279*, 208.
(13) Ha, T. H.; Koo, H. J.; Chung, B. H. *J. Phys. Chem. C* **2007**, *111*, 1123.
(14) Pan, Z. W.; Dai, Z. R.; Wang, Z. L. *Science* **2001**, *291*, 1947.
(15) Barnard, A. S.; Xiao, Y.; Cai, Z. *Chem. Phys. Lett.* **2006**, *419*, 313.
(16) Barnard, A. S. *J. Phys. Chem. B* **2006**, *110*, 24498.
(17) Fan, H. J.; Barnard, A. S.; Zacharias, M. *Appl. Phys. Lett.* **2007**, *90*, 143116.
(18) Zhang, L. G.; Jin, H.; Yang, W. Y.; Xie, Z. P.; Miao, H. H.; An, L. N. *Appl. Phys. Lett.* **2005**, *86*, 061908.
(19) Munakata, F.; Matsuo, K.; Furuya, K.; Akimune, Y.; Ye, J.; Ishikawa, I. *Appl. Phys. Lett.* **1999**, *74*, 3498.
(20) Zanatta, A. R.; Nunes, L. A. O. *Appl. Phys. Lett.* **1998**, *72*, 3127.
(21) Yang, W. Y.; Wang, H. T.; Liu, S. Z.; Xie, Z. P.; An, L. N. *J. Phys. Chem. B* **2007**, *111*, 4156.
(22) Zou, G. F.; Hu, B.; Xiong, K.; Li, H.; Dong, C.; Liang, J. B.; Qian, Y. T. *Appl. Phys. Lett.* **2005**, *86*, 181901.
(23) Xu, C. K.; Kim, M.; Chun, J.; Kim, D. E.; Chon, B.; Hong, S.; Joo, T. *Scripta Mater.* **2005**, *53*, 949.
(24) Zhang, J. Y.; Chen, Y. X.; Guo, T. L.; Lin, Z. X.; Wang, T. H. *Nanotechnology* **2007**, *18*, 325603.
(25) Krämer, M.; Wittmuss, D.; Kuppers, H.; Hoffmann, M. J.; Petzow, G. *J. Cryst. Growth* **1994**, *140*, 157.
(26) Yang, W. Y.; Xie, Z. P.; Li, J. J.; Miao, H. Z.; Zhang, L. G.; An, L. N. *J. Am. Ceram. Soc.* **2005**, *88*, 1647.
(27) Wang, Z. W.; Daemen, L. L.; Zhao, Y. S.; Zha, C. S.; Downs, R. T.; Wang, X. D.; Wang, Z. L.; Hemley, R. J. *Nat. Mater.* **2005**, *4*, 922.
(28) Yang, W. Y.; Xie, Z. P.; Miao, H. Z.; Zhang, L. G.; Ji, H.; An, L. N. *J. Am. Ceram. Soc.* **2005**, *88*, 466.

JP901938A